Supplementary Information

# Liposome fusion with orthogonal coiled coil peptides as fusogens: The efficacy of roleplaying peptides

Geert A. Daudey, Mengjie Shen, Ankush Singhal, Patrick van der Est, G.J. Agur Sevink, Aimee L. Boyle, and Alexander Kros*

Dept. Supramolecular Chemistry & Biomaterials, Leiden Institute of Chemistry, Leiden University, P.O. Box 9502, Leiden, 2300 RA, The Netherlands

E-mail: a.kros@chem.leidenuniv.nl

## Table of Contents

## Experimental section

### Materials

Fmoc-protected amino acids, rink amide resin, and O-(1H-6-Chlorobenzotriazole-1-yl)-1,1,3,3-tetramethyluronium hexafluorophosphate (HCTU) were purchased from NovaBioChem. Diisopropylethylamine (DIPEA), piperidine, acetic anhydride, N-methylpyrrolidine (NMP), dimethylformamide (DMF), acetonitrile, and trifluoroacetic acid (TFA) were obtained from Biosolve. Dichloromethane (DCM), diethyl ether, triisopropylsilane (TIS), trimethylamine (TEA), trifluoroethanol (TFE), cholesterol, trimethylphosphine (1M in toluene), (1H-benzotriazol-1-yloxy) tripyrrolidinophosphonium hexafluorophosphate (PyBOP), succinic anhydride, and sulphorhodamine B were obtained from Sigma Aldrich. 1,2-dioleoyl-sn-glycero-3-phosphatidylcholine (DOPC), and 1,2-dioleoyl-sn-glycero-3-phosphatidylethanolamine (DOPE) were purchased from Avanti polar lipids. The Fmoc–NH–$(PEG)_{12}$–COOH spacer was purchased from Iris Biotech. The $N_3$–$(PEG)_4$–COOH spacer[1,2] and Cholesteryl-4-amino-4-oxobutanoic acid[3] were synthesized according to literature procedures. PBS buffer contains 20 mM $PO_4^{3-}$ and 150 mM NaCl, pH 7.4. Sulphorhodamine B / PBS buffer contains 20 mM $PO_4^{3-}$, 130 mM NaCl and 20 mM Sulphorhodamine B, pH 7.4. Data analysis and visualization was performed using OriginPro 2017, Chimera 1.15rc and Chemdraw 20.0.

### Methods

**Liposome preparation.** A 1 mM stock solution containing DOPC/DOPE/cholesterol (50:25:25 mol%) in 1:1 (v/v) chloroform/methanol was prepared for all fusion experiments. For lipopeptides, 50 μM stock solutions were prepared using 1:1 (v/v) chloroform/methanol.

**Buffer containing liposomes.** 20 μL lipopeptide solution and 100 μL lipids solution were mixed (1 mol% lipopeptide) and the solvent was removed under a stream of $N_2$. The lipid/lipopeptide film was rehydrated with PBS (1 mL). The solution was briefly vortexed and subsequently sonicated for 5-10 minutes at 55 °C to yield ~100 nm diameter liposomes, verified with dynamic light scattering (DLS).[4] Solutions of buffer containing liposomes were used without further purification.

**Sulphorhodamine B loaded liposomes.** 60 μL lipopeptide solution and 300 μL lipids solution were mixed (1 mol% lipopeptide) and the solvent was removed under a stream of $N_2$. The lipid/lipopeptide film was rehydrated with PBS buffer containing 20 mM Sulphorhodamine B (0.7 mL). The solution was briefly vortexed and subsequently sonicated for 10-20 minutes at 55 °C to yield ~100 nm diameter liposomes. Non-encapsulated Sulphorhodamine B was removed using a Sephadex G25 column. Final liposome concentrations of 0.1 mM were obtained by further dilution with pure PBS (a 300 μL initial lipid solution gives 3 mL final liposome solution). Vesicle size distribution was verified with DLS after purification.[4]

Buffer containing or Sulphorhodamine B loaded plain liposomes are prepared as described above, with omission of the lipopeptide solutions.

**Fluorescence spectroscopy.** Content-mixing experiments were performed on a TECAN Infinite M1000 PRO fluorimeter using a 96-well plate at 24 °C. The percentage of fluorescence increase, *%F*, was calculated as:

$$\%F = \frac{F(t) - F_0}{F_{max} - F_0} * 100$$

where $F(t)$ is the fluorescence value at time *(t)*, $F_0$ is the initial fluorescence value and $F_{max}$ is the maximum fluorescence value. Initial and maximum values were determined for each experiment (content mixing or leakage control) and further details are provided in the sections below.

**Content mixing experiments.** The Sulphorhodamine B fluorescence intensity, $F(t)$, at 580 nm was monitored in a continuous fashion for 30 min after adding 100 µL of buffer containing liposomes (plain or functionalized with 1 mol% lipopeptide) to 100 µL of Sulphorhodamine B loaded liposomes (plain or functionalized with 1 mol% lipopeptide). $F_0$ was obtained by measuring the emission of 100 µL Sulphorhodamine B-loaded liposomes to which 100 µL of PBS was added, and $F_{max}$ was obtained by measuring the emission of a 200 µL solution of plain liposomes loaded with 10 mM Sulphorhodamine B. [Total lipid] = 0.1mM, in PBS pH 7.4, 24 °C.

**Leakage controls for content mixing experiments.** The Sulphorhodamine B fluorescence intensity, $F(t)$, at 580 nm was monitored in a continuous fashion for 30 min after mixing 100 µL of Sulphorhodamine B loaded liposomes (functionalized with 1 mol% lipopeptide) with 100 µL of Sulphorhodamine B loaded liposomes (functionalized with 1 mol% lipopeptide). The first point(s) after mixing served as $F_0$, while $F_{max}$ was obtained after completion of the experiment by addition of 10 uL Triton X-100 (10% solution in water).

**Dynamic Light Scattering.** Particle size distributions were measured by dynamic light scattering using a Malvern Zetasizer Nano ZS ZEN3500 equipped with a Peltier thermostatic cell holder. The laser wavelength was 633 nm and the scattering angle was 173°. The Stokes Einstein relationship

$$D = \frac{k_B T}{3\pi\eta D_h}$$

was used to estimate the hydrodynamic diameter $D_h$. Here, $k_B$ is the Boltzmann constant, $\eta$ is the solvent viscosity, and measurements were carried out at room temperature. Liposomal size was measured before and after the content mixing experiments.

**Circular Dichroism Spectroscopy.** CD spectra were obtained using a Jasco J-815 spectropolarimeter equipped with a peltier temperature controller. The ellipticity, given as mean residue molar ellipticity, $[\theta]$ (deg cm$^2$ dmol$^{-1}$), is calculated using the following equation

$$[\theta] = \frac{100 * \theta_{obs}}{nlc}$$

where $\theta_{obs}$ is the observed ellipticity (mdeg), *n* is the number of peptide residues, *l* is the path length of the cuvette (cm) and *c* is the peptide concentration (mM).

Spectra were recorded from 260 nm to 190 nm at 20 °C. Data points were collected with a 1 nm bandwidth at 1 nm intervals, using a scan speed of 1 nm s$^{-1}$. Each spectrum was an average of at least five scans. For analysis, each spectrum had the appropriate background spectrum (PBS or plain liposomes in PBS) subtracted. The percentage of α-helicity was calculated using the predicted value $[\theta]_{222}$ = -39500*(1-2.57/n) as 100% value for an α-helical peptide of n residues.[5] Spectral noise was defined as the standard deviation of a 5 nm window (x-2:x+2) and errors were estimated with 5% concentration deviations for both peptides and liposomes. For temperature dependent measurements, $[\theta]_{222}$ was recorded as a function of temperature, with a range of 2 – 80

°C and ΔT = 40°C/h. For experiments in the absence of vesicles, [total AcP] = 40 μM or 200 μM, in PBS, pH 7.4. For experiments in the presence of vesicles, [total lipid] = 0.5 mM or 1 mM, with [AcP] = 20 μM or 40 μM, or [lipopeptide] = 1, 2, 3 or 4 mol%, in PBS, pH 7.4. Precise used conditions are mentioned in the respective captions.

## Peptide synthesis

**Peptide synthesis:** Peptide synthesis was performed on a CEM Liberty I peptide synthesizer on a 100 μM scale using Rink amide resin (0.55-0.73 mmol/g). Amino acid activation was achieved using HCTU/DIPEA (4eq/6eq) in DMF. Fmoc-deprotection was carried out using two cycles of 20% piperidine in DMF. All reactions were carried out at 70-80 °C using microwave irradiation for three minutes.

**Acetylated peptides:** The N-terminal free amine was acetylated using a mixture of $Ac_2O$ (50 mM) and DIPEA (12.5 mM) in NMP.

**Lipopeptides:** The $N_3$-Peg$_4$-COOH and FmocNH-Peg$_{12}$-COOH spacers were conjugated to the peptide free N-termini using PyBOP/DIPEA activation (3eq/5eq) in DMF containing LiCl (1mg/mL) for 2h. $N_3$-PEG$_4$ containing peptides were reduced to primary amines using two cycles of $PMe_3$ in dioxane/water (4:1). FmocNH-Peg$_{12}$ conjugated peptides were deprotected to obtain the primary amines using two cycles of 20% piperidine in DMF. Cholesteryl-4-amino-4-oxobutanoic acid was activated with PyBOP/DIPEA (3eq/5eq) in DCM/DMF 1:1, added to the resin-bound peptides and the reaction was shaken for two days at rt. The resin was washed thoroughly with DMF and DCM to remove excess reactants.

**Cleavage:** The (lipo)peptides were cleaved from the resin and side-chain deprotected using a mixture of TFA/TIS/$H_2O$ (95:2.5:2.5 v/v) for 2h. The (lipo)peptides were precipitated in cold diethyl ether followed by centrifugation and dried under vacuum.

**Purification:** RP-HPLC was performed with a Shimadzu HPLC system with two LC-8A pumps, and a SPD-10AVP UV-VIS detector. Sample elution was monitored by UV detection at 214 nm and 278 nm. Samples were eluted with a linear gradient from 10% to 90% (v/v) B in A, A being $H_2O$, 0.1% (v/v) TFA, and B being MeCN, 0.1% (v/v) TFA. Purification of (lipo)peptides was performed on a Phenomenex C18 reversed phase column (21.2 mm diameter, 150 mm length, 5.00 μM particle size) with a flow rate of 15 mL min$^{-1}$. Collected fractions were tested for >95% purity using LC-MS with Gemini C18 column and freeze dried.

## Peptide analysis

Peptide purity was confirmed using LC-MS analysis equipped with Gemini 3μ C18 column coupled with Finningan LCQ advantage max (Thermo) ESI-MS analyzer and the results are summarized in Table S1-S2. LCMS eluents were A) $H_2O$ + 0.1% v/v TFA, B) MeCN + 0.1% v/v TFA, with a flow rate of 1 mL min$^{-1}$. Gradient for acetylated peptides was applied from 2 to 30 min, from 10% B in A to 90% B in A, while the same gradient was applied for lipopeptides from 1 to 12 min. Retention time Rt is rounded to 2 significant numbers.

**Table S1. Analysis of AcP Peptides**

| Peptide | Formula | Calc. mass | Observed mass | Rt (min) | Isoelectric point[a] | Charge[a] |
|---|---|---|---|---|---|---|
| AcP1$_E$ | $C_{140}H_{219}N_{35}O_{56}$ | 3288.458 | 3312.325 $[M+Na]^+$ | 22 | 2.78 | -10.0 |
| AcP1$_K$ | $C_{150}H_{261}N_{43}O_{42}$ | 3338.963 | 3340.463 $[M+H]^+$ | 12 | 10.40 | +4.8 |
| AcP2$_E$ | $C_{146}H_{242}N_{40}O_{49}$ | 3341.744 | 3343.847 $[M+H]^+$ | 19 | 4.62 | -2.1 |
| AcP2$_K$ | $C_{146}H_{243}N_{41}O_{48}$ | 3340.759 | 3342.646 $[M+H]^+$ | 16 | 4.92 | -1.1 |
| AcP3$_E$ | $C_{144}H_{238}N_{38}O_{49}$ | 3285.677 | 3287.231 $[M+H]^+$ | 20 | 4.44 | -3.1 |

| | | | | | | |
|---|---|---|---|---|---|---|
| AcP3$_K$ | $C_{142}H_{236}N_{38}O_{47}$ | 3227.641 | 3229.010 $[M+H]^+$ | 18 | 4.62 | -2.1 |
| AcP4$_E$ | $C_{144}H_{239}N_{39}O_{48}$ | 3284.692 | 3287.046 $[M+H]^+$ | 17 | 4.62 | -2.1 |
| AcP4$_K$ | $C_{146}H_{242}N_{40}O_{49}$ | 3341.744 | 3344.621 $[M+H]^+$ | 16 | 4.62 | -2.1 |

**[a] Calculated with Isoelectric Point Calculator and peptide charge is calculated at pH 7.4.**

**Table S2. Analysis of synthesized lipopeptides**

| Peptide | Formula | Calc mass | Observed mass | Rt (min) |
|---|---|---|---|---|
| Cpeg$_4$P1$_E$ | $C_{179}H_{284}N_{36}O_{63}$ | 3948.36 | 1974.80 $[M+2H]^{2+}$ | 11 |
| Cpeg$_4$P1$_K$ | $C_{189}H_{326}N_{44}O_{49}$ | 3998.86 | 1357.73 $[M+3Na]^{3+}$ | 7.4 |
| Cpeg$_4$P2$_E$ | $C_{185}H_{307}N_{41}O_{56}$ | 4001.65 | 1335.00 $[M+3H]^{3+}$ | 9.2 |
| Cpeg$_4$P2$_K$ | $C_{185}H_{308}N_{42}O_{55}$ | 4000.66 | 1334.60 $[M+3H]^{3+}$ | 8.6 |
| Cpeg$_4$P3$_E$ | $C_{183}H_{303}N_{39}O_{56}$ | 3945.58 | 1973.47 $[M+2H]^{2+}$ | 8.7 |
| Cpeg$_4$P3$_K$ | $C_{181}H_{301}N_{39}O_{54}$ | 3887.54 | 1944.27 $[M+2H]^{2+}$ | 9.0 |
| Cpeg$_4$P4$_E$ | $C_{183}H_{304}N_{40}O_{55}$ | 3944.59 | 1973.53 $[M+2H]^{2+}$ | 9.6 |
| Cpeg$_4$P4$_K$ | $C_{185}H_{307}N_{41}O_{56}$ | 4001.65 | 1334.93 $[M+3H]^{3+}$ | 9.3 |
| Cpeg$_{12}$P1$_E$ | $C_{196}H_{318}N_{36}O_{71}$ | 4314.81 | 1438.87 $[M+3H]^{3+}$ | 9.6 |
| Cpeg$_{12}$P1$_K$ | $C_{206}H_{360}N_{44}O_{57}$ | 4365.31 | 1455.73 $[M+3H]^{3+}$ | 6.9 |
| Cpeg$_{12}$P2$_E$ | $C_{202}H_{341}N_{41}O_{64}$ | 4368.09 | 1456.40 $[M+3H]^{3+}$ | 7.6 |
| Cpeg$_{12}$P2$_K$ | $C_{202}H_{342}N_{42}O_{63}$ | 4367.11 | 1456.13 $[M+3H]^{3+}$ | 7.5 |
| Cpeg$_{12}$P3$_E$ | $C_{200}H_{337}N_{39}O_{64}$ | 4312.03 | 1437.73 $[M+3H]^{3+}$ | 7.5 |
| Cpeg$_{12}$P3$_K$ | $C_{198}H_{335}N_{39}O_{62}$ | 4253.99 | 1418.47 $[M+3H]^{3+}$ | 7.6 |
| Cpeg$_{12}$P4$_E$ | $C_{200}H_{338}N_{40}O_{63}$ | 4311.04 | 1437.40 $[M+3H]^{3+}$ | 7.5 |
| Cpeg$_{12}$P4$_K$ | $C_{202}H_{341}N_{41}O_{64}$ | 4368.09 | 1456.53 $[M+3H]^{3+}$ | 7.5 |

## Peptide linker structures, Hydrophobic core and Helical wheel representations

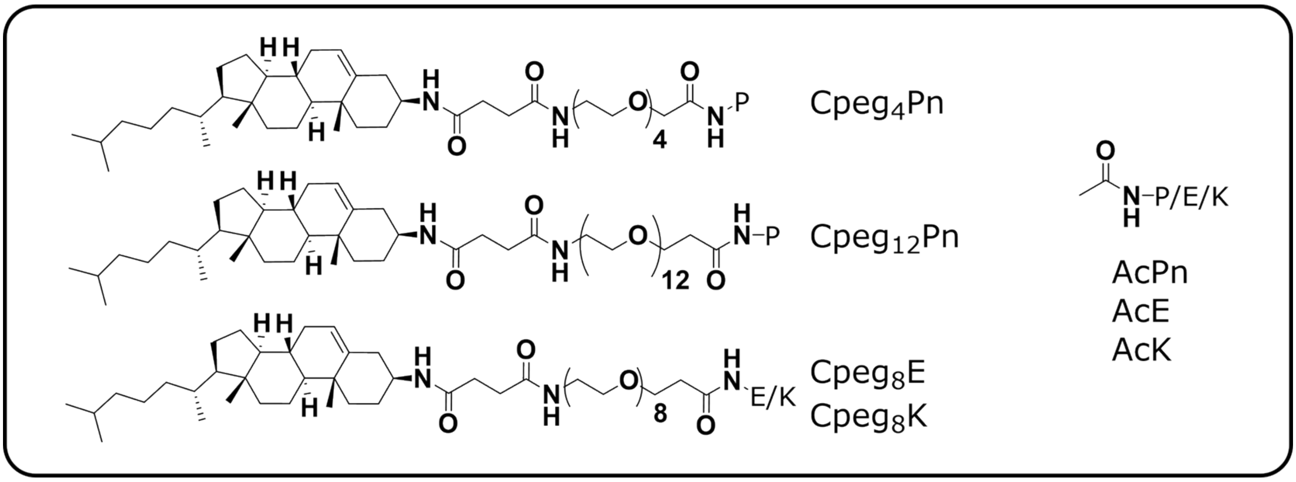


**Figure S1. Molecular structure of used linkers, functional peptide fusogens were obtained using PEG4, PEG8 and/or PEG12 linkers.**

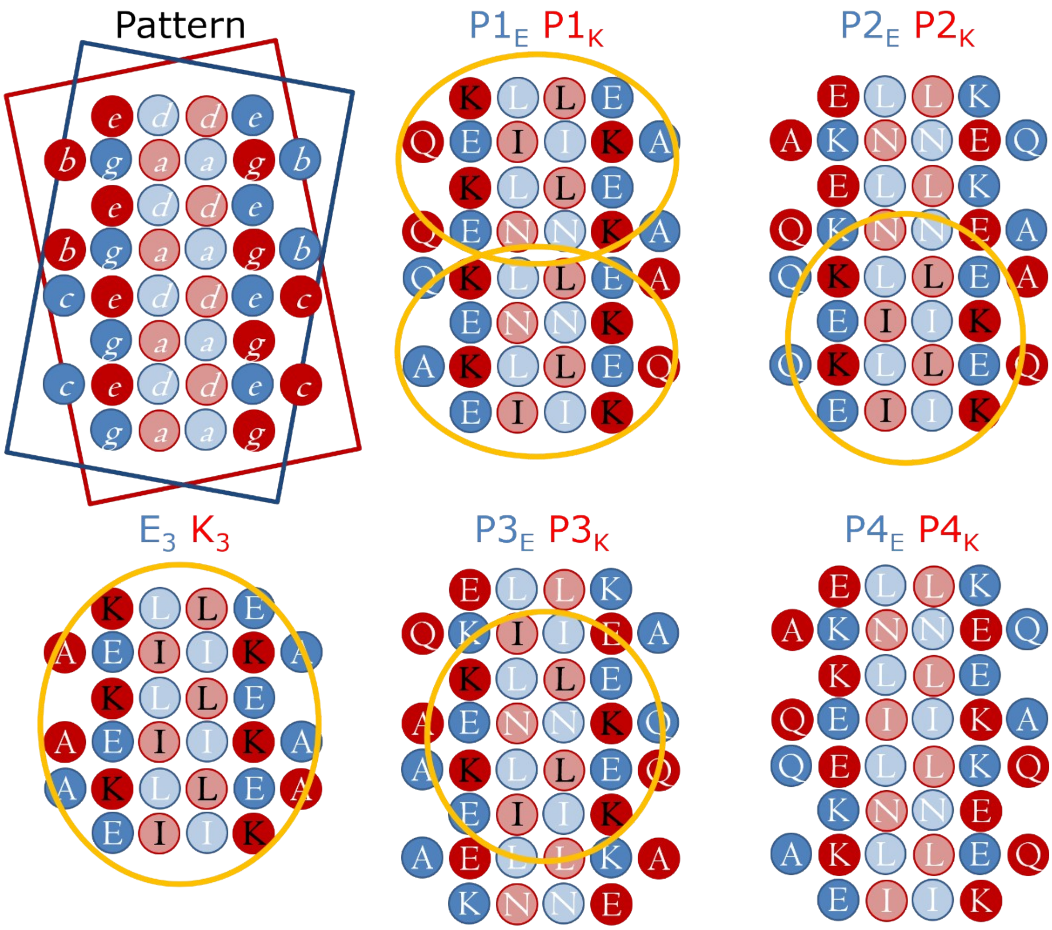


**Figure S2. Hydrophobic core interface of the designed CC pairs with the ´E´ peptide depicted in blue and ´K´ peptide in red. Yellow circles mark the Amphiphatic class A patterns of the ´K´ peptides with at least four positive charged Lys (K) residues next to the hydrophobic core consisting of two Leu (L) and at least one Ile (I) residue which are highlighted in black for clarity. The 'K' peptides are visualized from the inside of the α-helix, i.e. mirror images. The top first image shows the pattern with the precise amino acid positions and the two squares illustrate the tilting of the two CC helices. N-termini are located on the bottom.**

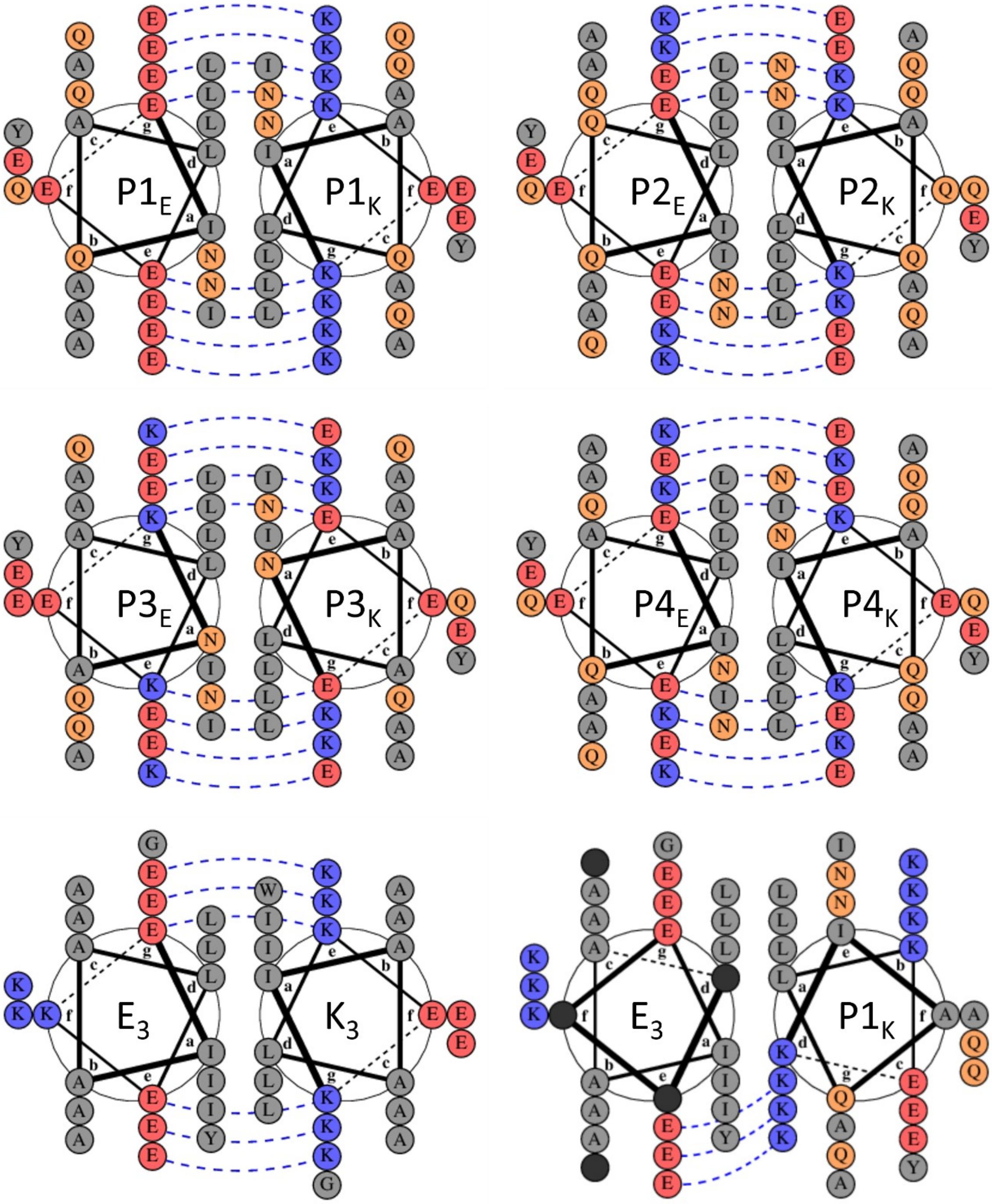


**Figure S3. Helical wheel projection of the CC pairs. Asn (N) and Ile (I) are both inserted twice in the hydrophobic core of each CC pair at position a, with different positions for the individual orthogonal pairs thereby enhancing pairing specificity. For electrostatic interactions at positions e and g, Glu (E) and Lys (K) were used as charged residues,6 with opposite charges at complementary heptads within the paired heterodimer. The electrostatic patterns along the CC complex differ also for all orthogonal pairs, contributing to partner specificity. $E_3$ $(EIAALEK)_3$ and $K_3$ $(KIAALKE)_3$ are also shown for comparison. Graphs made using Drawcoil 1.0.**

## CD Measurements

### CD spectra of intermolecular peptide interactions in pure PBS

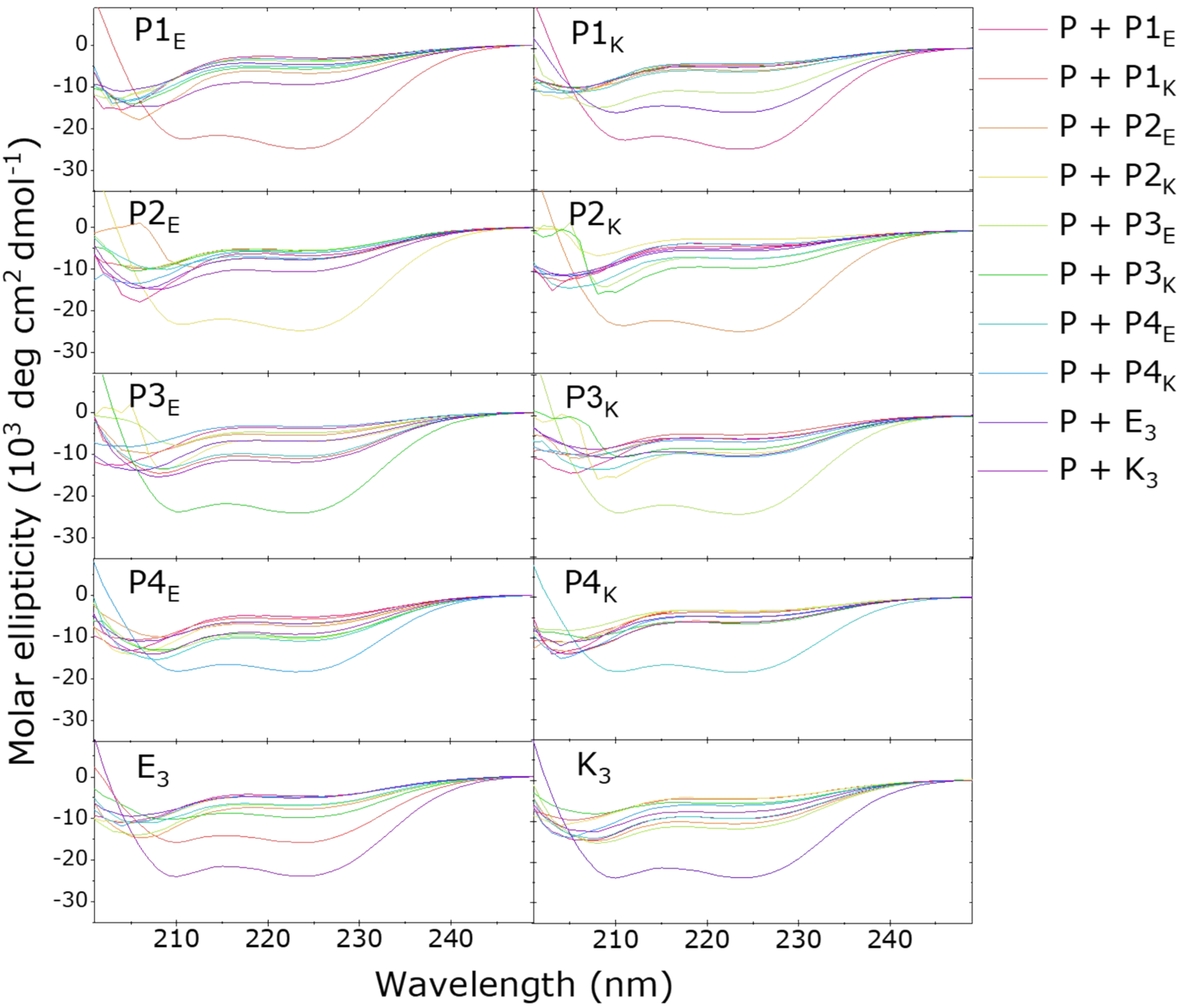


**Figure S4. CD spectra of combinations of peptides Pn, $E_3$, and $K_3$ in PBS buffer to determine heteromeric peptide interactions. [Total peptide] = 200 µM, in PBS pH 7.4.**

**Table S3. $\theta_{222}/\theta_{208}$ ratio of all peptide combinations**

| Peptide | $P1_E$ | $P1_K$ | $P2_E$ | $P2_K$ | $P3_E$ | $P3_K$ | $P4_E$ | $P4_K$ | $E_3$ | $K_3$ |
|---|---|---|---|---|---|---|---|---|---|---|
| $K_3$ | 0.64 | 0.85 | 0.72 | 0.39 | 0.77 | 0.69 | 0.66 | 0.45 | 1.00 | 0.63 |
| $E_3$ | 0.42 | 0.99 | 0.53 | 0.43 | 0.50 | 0.96 | 0.62 | 0.41 | 0.48 | |
| $P4_K$ | 0.24 | 0.34 | 0.46 | 0.27 | 0.41 | 0.65 | 1.01 | 0.32 | | |
| $P4_E$ | 0.39 | 0.54 | 0.74 | 0.47 | 0.78 | 0.77 | 0.71 | | | |
| $P3_K$ | 0.41 | 0.49 | 0.55 | 0.63 | 1.01 | 0.82 | | | | |
| $P3_E$ | 0.30 | 0.76 | 0.56 | 0.49 | 0.62 | | | | | |
| $P2_K$ | 0.25 | 0.33 | 1.06 | 0.34 | | | | | | |
| $P2_E$ | 0.38 | 0.55 | 0.80 | | | | | | | |
| $P1_K$ | 1.10 | 0.39 | | | | | | | | |
| $P1_E$ | 0.20 | | | | | | | | | |

**Measured $\theta_{222}/\theta_{208}$ ratio of all possible combinations of N-acetylated peptides $Pn_E$, $Pn_K$, $E_3$ and $K_3$ as calculated from the spectra shown in Figure S4. Values ≥1 are characteristic for CC formation. [Total peptide] = 200 µM, PBS pH 7.4, 20 °C.**

**Table S4. Helicity of equimolar peptide combinations**

| Peptide | $P1_E$ | $P1_K$ | $P2_E$ | $P2_K$ | $P3_E$ | $P3_K$ | $P4_E$ | $P4_K$ | $E_3$ | $K_3$ |
|---|---|---|---|---|---|---|---|---|---|---|
| $K_3$ | 24 | 10 | 27 | 10 | 31 | 14 | 24 | 15 | 52 | 15 |
| $E_3$ | 11 | 42 | 19 | 12 | 17 | 25 | 17 | 11 | 9 | |
| $P4_K$ | 7 | 9 | 15 | 8 | 8 | 16 | 49 | 11 | | |
| $P4_E$ | 13 | 14 | 19 | 17 | 27 | 26 | 29 | | | |
| $P3_K$ | 14 | 11 | 11 | 19 | 65 | 22 | | | | |
| $P3_E$ | 9 | 29 | 10 | 14 | 13 | | | | | |
| $P2_K$ | 8 | 9 | 67 | 5 | | | | | | |
| $P2_E$ | 17 | 13 | 21 | | | | | | | |
| $P1_K$ | 67 | 10 | | | | | | | | |
| $P1_E$ | 7 | | | | | | | | | |

**Percentage α-helicity was calculated from the spectra shown in Figure S4 using the formula $[\theta]_{222}$=-39500*(1-2.57/n) to obtain the 100% helicity value for an α-helical peptide of *n* residues. [Total peptide] = 200 µM, PBS pH 7.4 at 20 °C.**

**Table S5. Found absolute %helicity deviation (%ΔH) from calculated average helicity of equimolar peptide combinations**

| Peptide | $P1_E$ | $P1_K$ | $P2_E$ | $P2_K$ | $P3_E$ | $P3_K$ | $P4_E$ | $P4_K$ | $E_3$ | $K_3$ |
|---|---|---|---|---|---|---|---|---|---|---|
| $K_3$ | 13 | -2 | 10 | 0 | 17 | -5 | 2 | 2 | 40 | 0 |
| $E_3$ | 3 | 32 | 5 | 5 | 6 | 9 | -2 | 1 | 0 | |
| $P4_K$ | -2 | -2 | -1 | -1 | -4 | -1 | 29 | 0 | | |
| $P4_E$ | -5 | -5 | -6 | 0 | 7 | 1 | 0 | | | |
| $P3_K$ | -1 | -5 | -10 | 5 | 48 | 0 | | | | |
| $P3_E$ | -1 | 17 | -6 | 5 | 0 | | | | | |
| $P2_K$ | 2 | 2 | 54 | 0 | | | | | | |
| $P2_E$ | 3 | -2 | 0 | | | | | | | |
| $P1_K$ | 58 | 0 | | | | | | | | |
| $P1_E$ | 0 | | | | | | | | | |

## Temperature and concentration dependent unfolding curves

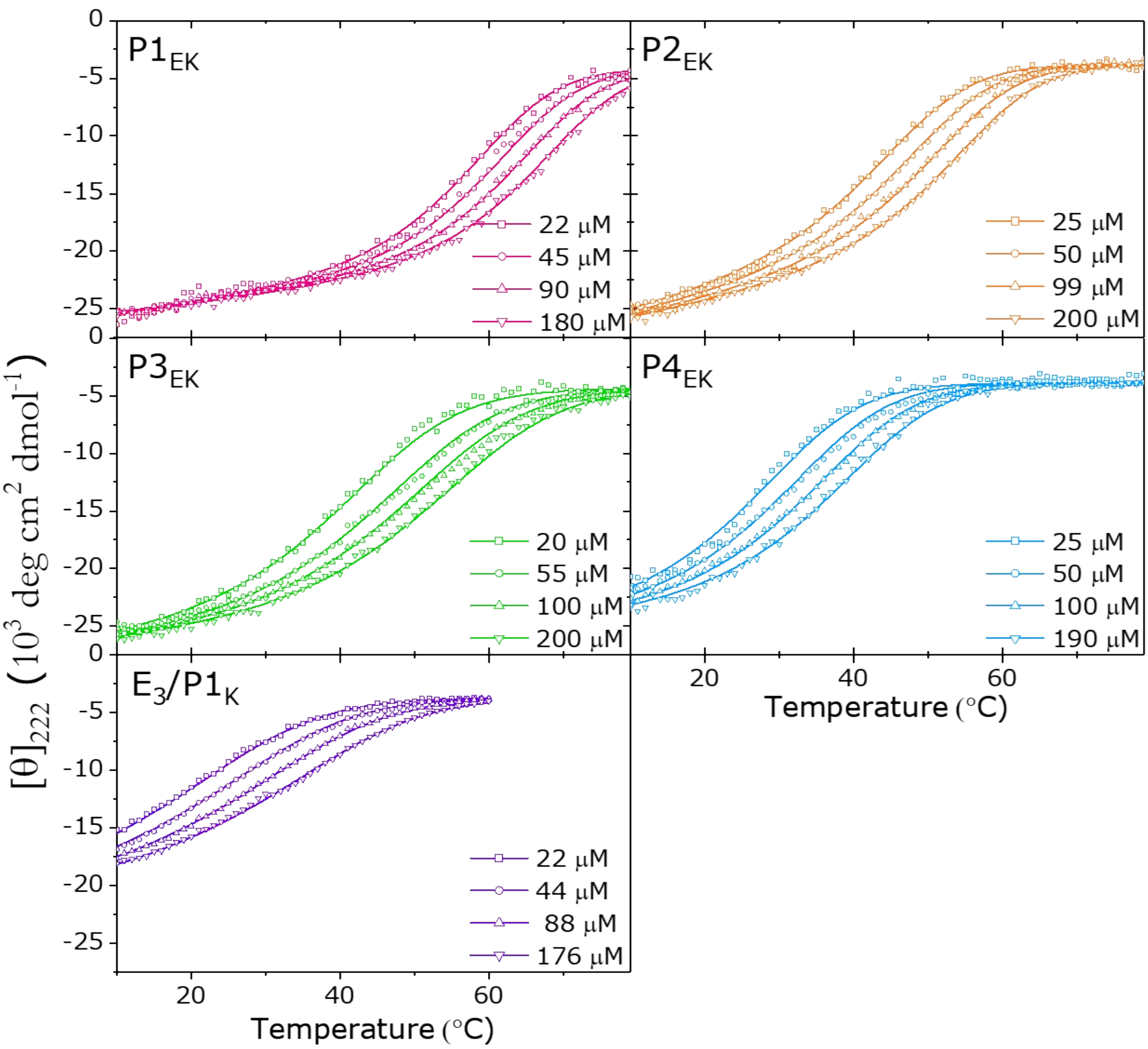


**Figure S5. Concentration dependent thermal unfolding of designed heterodimers $P1_{EK}$, $P2_{EK}$, $P3_{EK}$, $P4_{EK}$ and $E_3/P1_K$. Best fits (lines) of experimental data (dots) are obtained using *FitDis!*. Measured in pure PBS, pH 7.4.**

**Table S6. Parameters for formal description of CC complexes**

| CC-complex | $P1_{EK}$ | $P2_{EK}$ | $P3_{EK}$ | $P4_{EK}$ | $E_3/K_3$ [c] | $E_3/P1_K$ |
|---|---|---|---|---|---|---|
| $P_{Tmin} – P_{Tmax}$ / μM [a] | 22 – 180 | 25 – 200 | 20 – 200 | 25 – 190 | 3 – 25 | 44 – 380 |
| Found $\upsilon_1$, $\upsilon_2$, $\upsilon_3$,. [b] | 1,1 | 1,1 | 1,1 | 1,1 | 1,1 | 1,1 |
| Tm / °C (200 μM) | 63 | 50 | 51 | 37 | 67 | 32 |
| ΔH° / kJ mol$^{-1}$ | 282 | 281 | 171 | 194 | 215 | 163 |
| T° / °C | 107 | 92 | 114 | 88 | 144 | 92 |
| $\Delta C_P$ / kJ mol$^{-1}$ K$^{-1}$ | 1.6 | 2.5 | 0.3 | 0.8 | 1.1 | 0.8 |
| $\theta_{F0}$ / $10^3$ | -26.2 | -27.3 | -27.0 | -24.7 | -29.9 | -20.7 |
| $m_{F0}$ | 78.2 | 113.4 | 84.8 | 60.4 | 94.5 | 76.4 |
| $\theta_{U0}$ / $10^3$ | -4.1 | -3.8 | -4.4 | -3.9 | -5.8 | -3.7 |
| $m_{U0}$ | (0) | (0) | (0) | (0) | 4 | (0) |

**[a] range of total peptide complex concentration used in experiment. [b] stoichiometric factors of best fitting model. [c] taken from M. Rabe et al.[7]**

**CD spectra of peptides tethered to liposomes with increasing [CPeg$_4$Pn].**

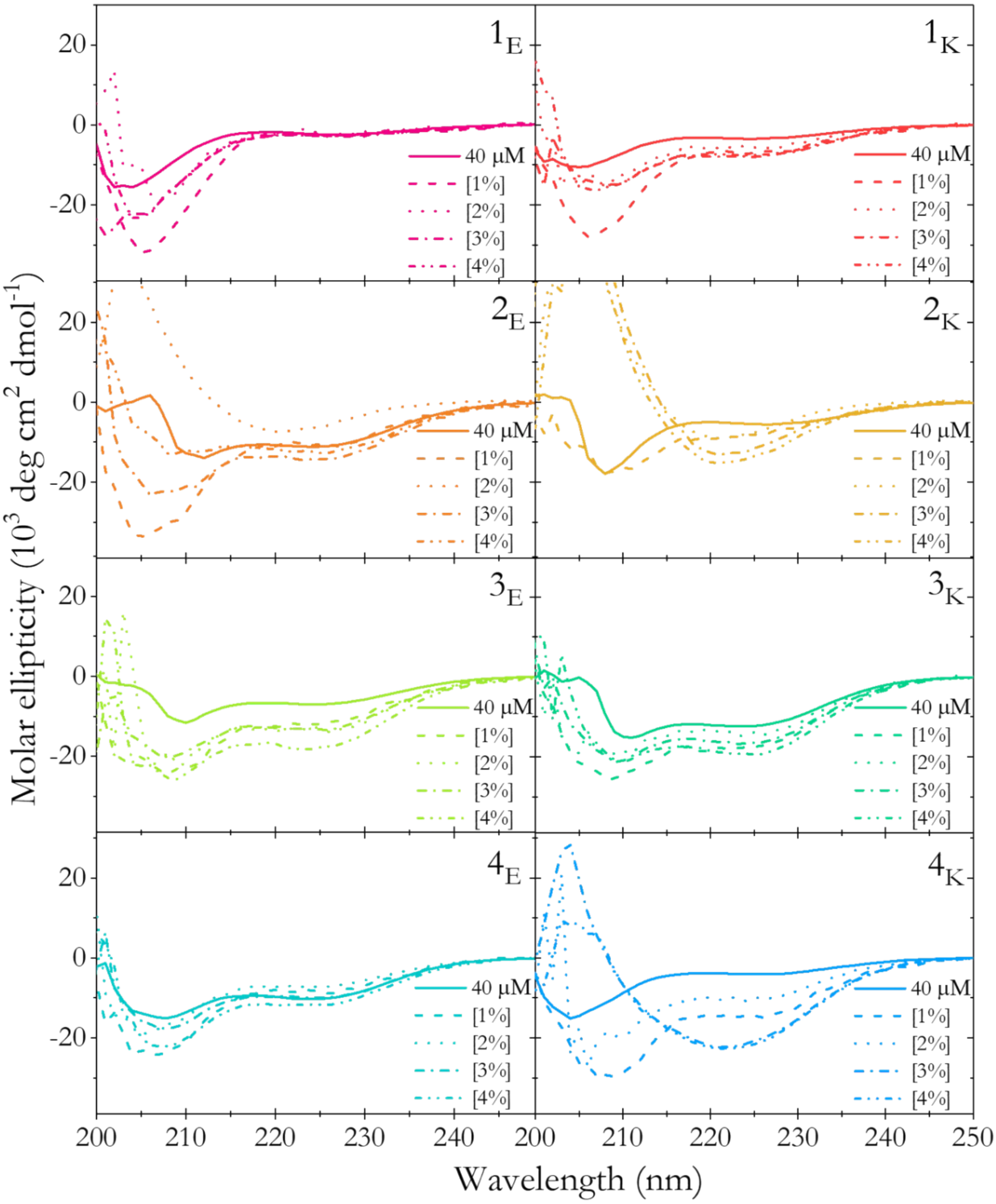


**Figure S6. CD spectra of peptides tethered to liposomes with increasing [CPeg$_4$Pn], with acetylated peptide AcPn in the absence of liposomes (40 µM, solid line) as reference. [Total lipid] = 0.5 mM, with 5, 10, 15, 20 µM lipopeptide, in PBS pH 7.4 at 20 °C.**

## Thermal unfolding curves of membrane tethered lipopeptides

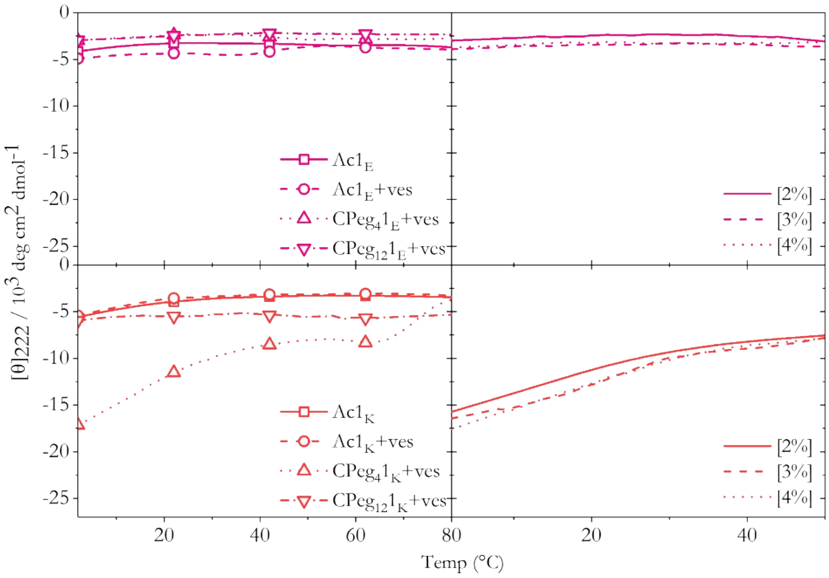


**Figure S7. Melting curves of $P1_E$ and $P1_K$ peptides. Left: with acetylated peptides in the absence and presence of vesicles, and with lipopeptide decorated liposomes. Right: with increasing [Cpeg$_4$P1]. [Total lipid] + [AcP1] = 1 mM + 20 µM. [Total lipid] + [ Cpeg$_{4/12}$P1] = 0.5 mM + 10, 15, or 20 µM, in PBS pH 7.4.**

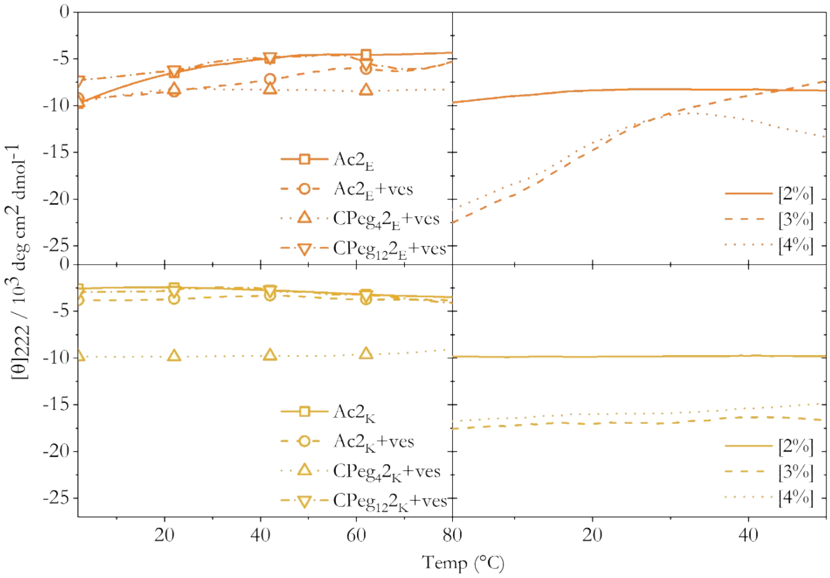


**Figure S8. Melting curves of $P2_E$ and $P2_K$ peptides. Left: with acetylated peptides in the absence and presence of vesicles, and with lipopeptide decorated liposomes. Right: with increasing [CPeg$_4$P2]. [Total lipid] + [AcP2] = 1 mM + 20 µM. [Total lipid] + [Cpeg$_{4/12}$P2] = 0.5 mM + 10, 15, or 20 µM, in PBS pH 7.4.**

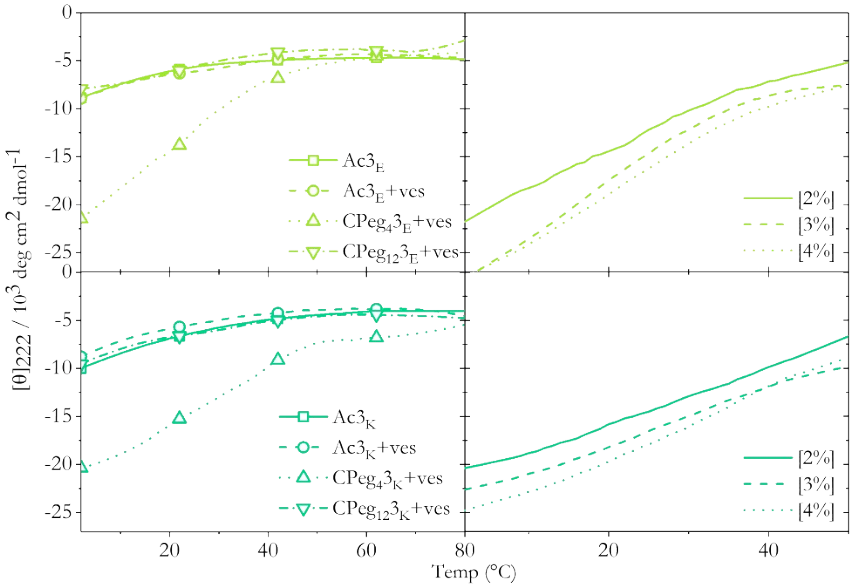


**Figure S9. Melting curves of $P3_E$ and $P3_K$ peptides. Left: with acetylated peptides in the absence and presence of vesicles, and with lipopeptide decorated liposomes. Right: with increasing [$Cpeg_4P3$]. [Total lipid] + [AcP3] = 1 mM + 20 µM. [Total lipid] + [$Cpeg_{4/12}P3$] = 0.5 mM + 10, 15, or 20 µM, in PBS pH 7.4.**

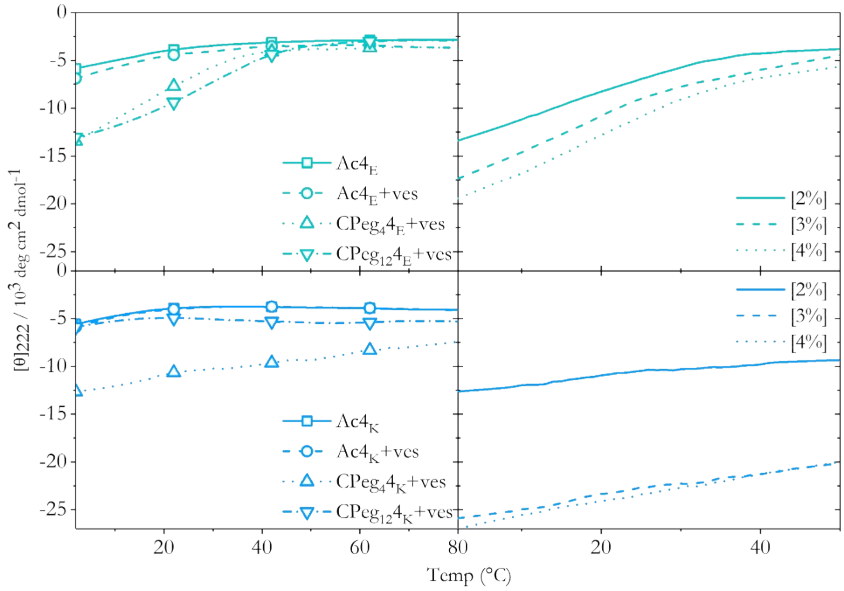


**Figure S10. Melting curves of $P4_E$ and $P4_K$ peptides. Left: with acetylated peptides in the absence and presence of vesicles, and with lipopeptide decorated liposomes. Right: with increasing [$Cpeg_4P4$]. [Total lipid] + [AcP4] = 1 mM + 20 µM. [Total lipid] + [$Cpeg_{4/12}P4$] = 0.5 mM + 10, 15, or 20 µM, in PBS pH 7.4.**

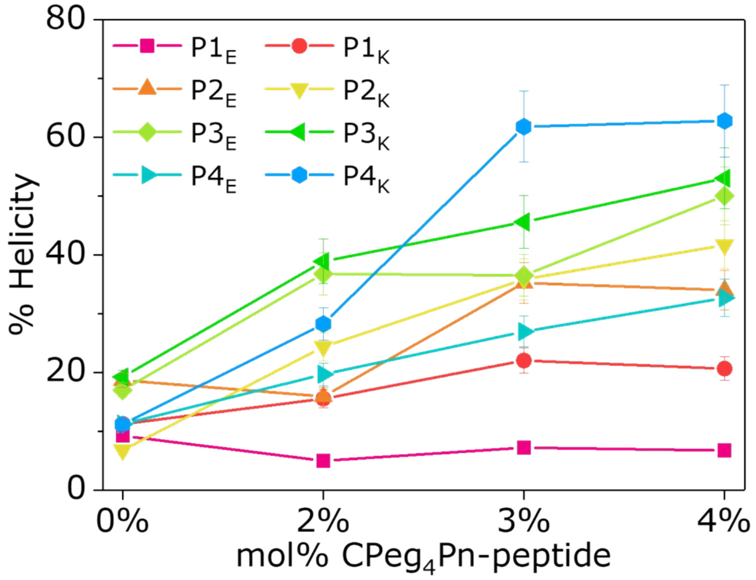


**Figure S11.** Helicity of peptides tethered to liposomes with increasing [Cpeg$_4$Pn], taken from melting curves at 20 °C. The first entry contains helicity of AcPn-peptides in the presence of liposomes. [total lipid] + [AcPn] = 1 mM + 20 µM; [total lipid] = 0.5 mM; with [Cpeg$_4$Pn] = 10, 15, or 20 µM, in PBS pH 7.4 at 20 °C.

## CC interaction between peptide functionalized liposomes

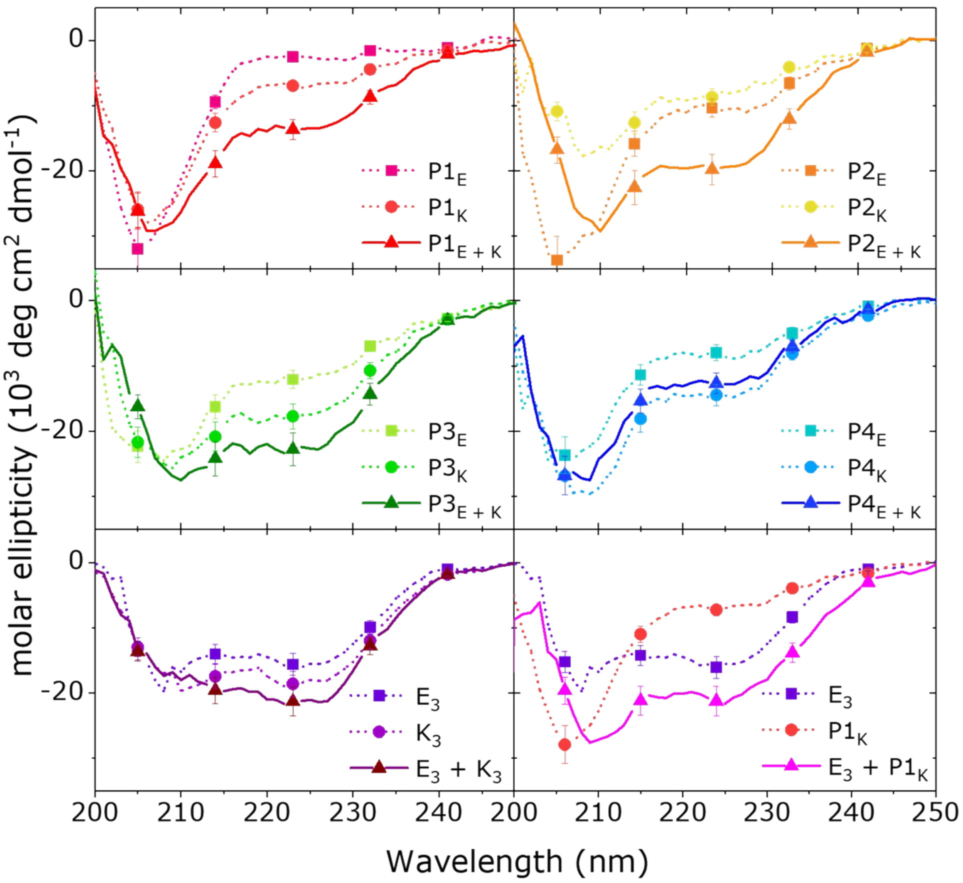


**Figure S12.** CD spectra of liposomes decorated with Cpeg$_4$Pn or Cpeg$_8$E$_3$/K$_3$, and the equimolar mixture of liposomes bearing complementary peptides. [Total lipid] = 0.5 mM, with 1 mol% lipopeptide, PBS pH 7.4, 20 °C. Error bars represent 5% concentration deviation for peptides and liposomes, and spectral noise.

## Content mixing assay

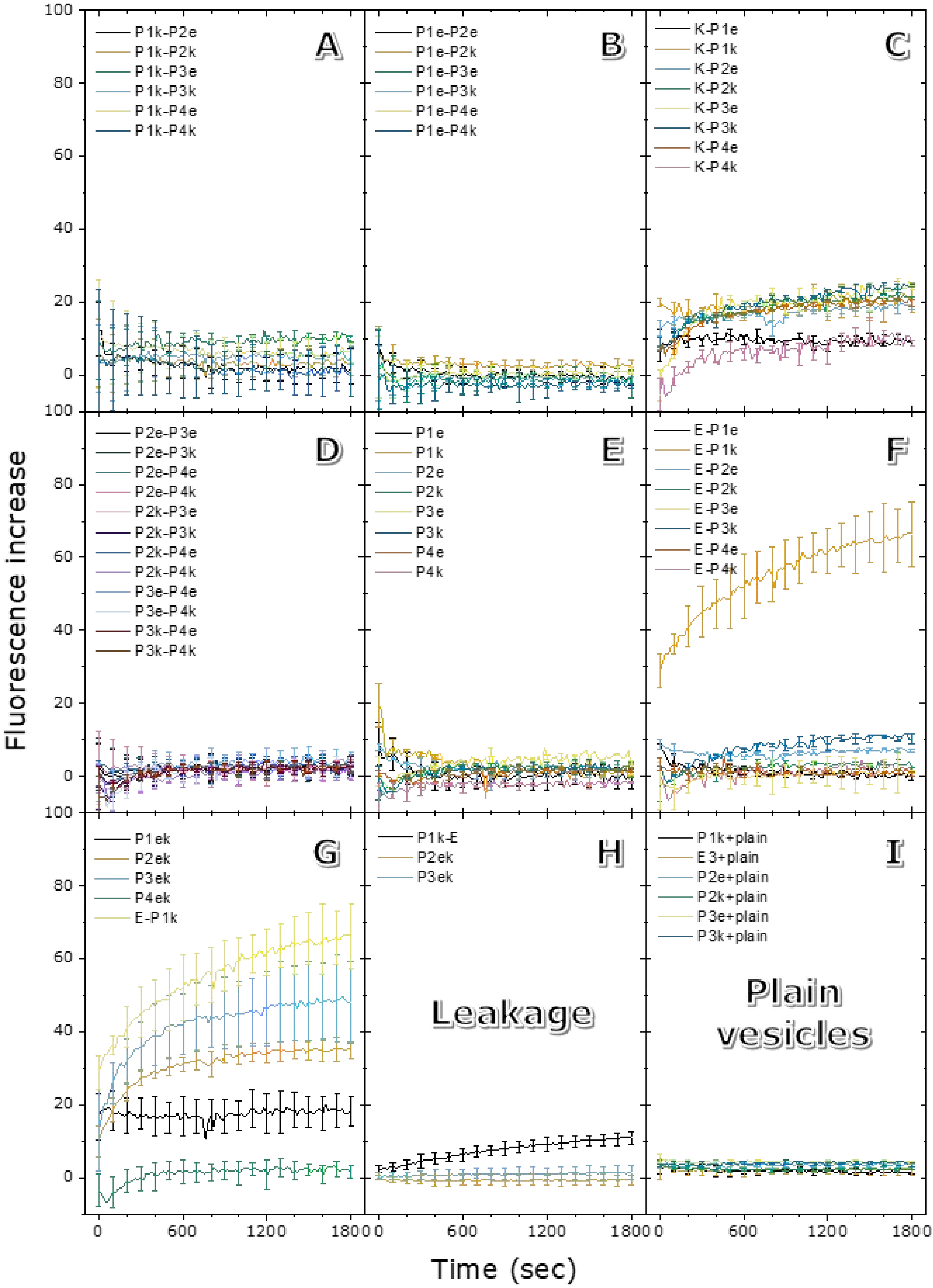


**Figure S13. Content mixing assay of liposomes functionalized with Cpeg$_4$Pn or Cpeg$_8$E$_3$/Cpeg$_8$K$_3$. (A,B,D,E) All non-pair- or homomeric combinations of Pn peptides. (C,F) Non-pair combinations of Pn with E$_3$ and K$_3$. (G) Content mixing of designed Pn$_{EK}$ pairs and E$_3$/P1$_K$. (H) Leakage assay of most fusogenic (>30% efficiency) peptide pairs E$_3$/P1$_K$, P2$_{EK}$ and P3$_{EK}$. (I) Control experiments with bare liposomes and the individual peptides of the fusogenic sets E$_3$/P1$_K$, P2$_{EK}$ and P3$_{EK}$. [Total lipid] = 0.1 mM with 1 mol% lipopeptide in PBS pH 7.4 at 25 °C. Fusion profiles are averages of triplicates.**

## DLS experiments

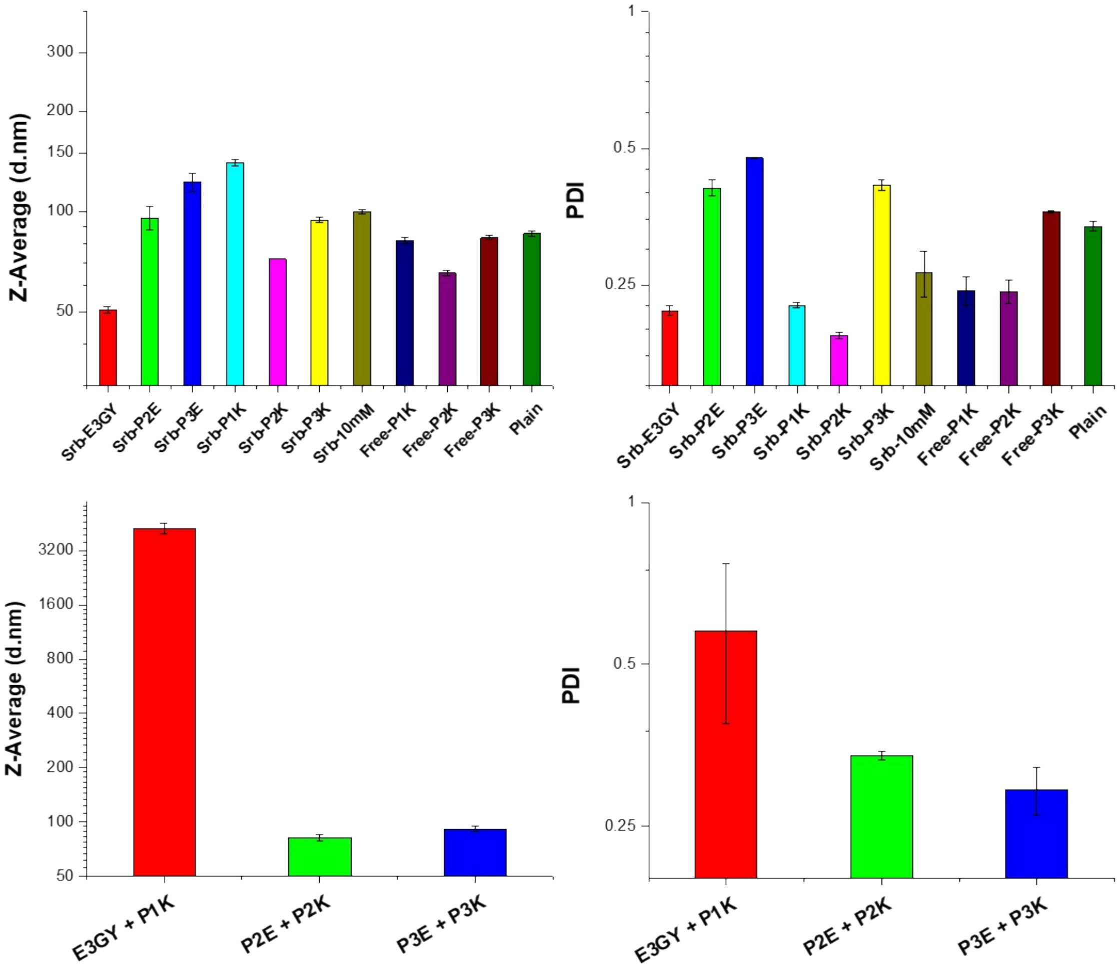


**Figure S14. DLS measurements of liposomes before (top) and after the fusion assay (bottom). Vesicle size is slightly affected by the used lipopeptide and the presence or absence of 20mM Sulphorhodamine B loading. Significant size increase upon mixing of $P1_K$ and $E_3$ functionalized liposomes is evident, while the efficient fusogens $P2_{EK}$ and $P3_{EK}$ do not induce massive size increase.**

## Molecular Dynamics Simulation setup

The initial structures of the $E_3$/$K_3$ peptides were taken from the PDB database (1U0I).[8] The $K_3$ peptide was modified to form $P1_K$ using the PYMOL peptide builder.[9] All simulations were performed at atomic resolution, in a solvated cubic box of dimension 9x9x9 $nm^3$, using GROMACS 2016.[10] Both N-termini were capped with an acetyl residue and the C-termini with an amide residue. Two different $P1_K$ and $E_3$ heterodimer starting configurations were considered: (i) a parallel CC with the N-terminus of $P1_K$ in the proximity of the N-terminus of $E_3$, (ii) an antiparallel CC with the N-terminus of $P1_K$ in the proximity of the C-terminus of $E_3$. The CHARMM36 force field[11] was used for both peptides and the TIP3P[12] model for the water molecules. All hydrogen atoms were constrained with the LINCS algorithm,[13] and long-range electrostatics were evaluated with particle-mesh Ewald summation.[14] All simulations used Leap-Frog integrator[15] with 2 fs timestep and 1.4 nm cutoff was used for all the interactions. A standard energy minimization procedure with the steepest descent method[16] was employed. Subsequently, a 300 ns NPT equilibration run was performed using a Nose-Hoover thermostat[17] at 300 K and Parrinello−Rahman barostat[18] at 1 atm, followed by a 600 ns production MD run.

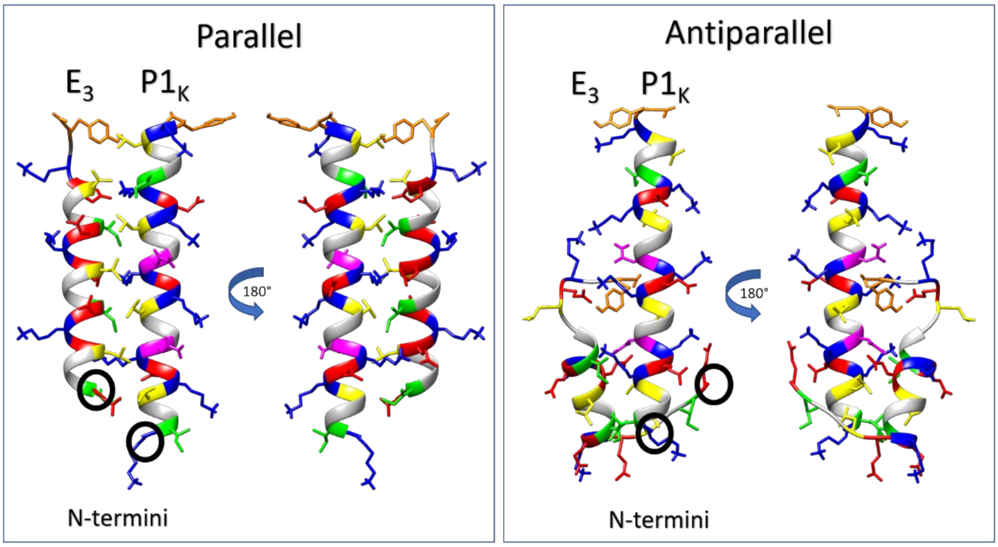


**Figure S15. Snapshots of final structures obtained by MD simulations. Colour guide: Leu (yellow), Ile (green), Lys (blue), Glu (red), Asn (purple), and C-terminal Tyr (orange). Ala, Gly and Gln are depicted in white, without side chains for clarity. N termini are highlighted once with a black circle.**

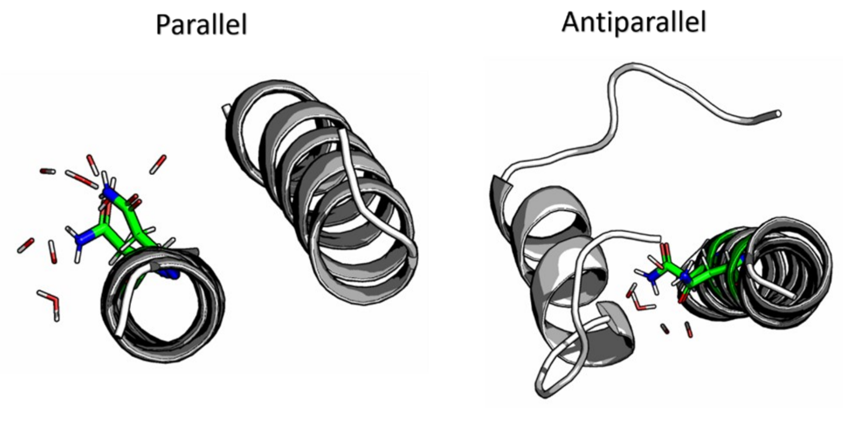


**Figure S16. Snapshots of final structures obtained by MD simulations showing the associated water molecules of both Asn residues. View along the helical axis of $P1_K$ with the C-terminus in the front.**

## SOCKET analysis of $E_3/P1_K$: Knobs-into-holes assignment

```
SOCKET v3.02 02-11-01 John Walshaw, University of Sussex
using cutoff of  8.0 Angstroms for centre of mass distances

These are the knobs and holes:

knobs in helix 0:
0) 6 (LYS 9: , iCode=' ', helix 0) type 4 (hole:  ILE 43:  iCode=' ', LEU 46: iCode=' ', GLU 47: iCode=' ', ILE 50: iCode=' ' helix 1) packing angle  93.250
1) 10 (LEU 13: , iCode=' ', helix 0) type 4    (hole:  LEU 46:  iCode=' ', GLU 49:  iCode=' ', ILE 50:  iCode=' ', LEU 53:  iCode=' ' helix 1) packing angle 24.518
2) 13 (LYS 16: , iCode=' ', helix 0) type 3    (hole:  ILE 50:  iCode=' ', LEU 53:  iCode=' ', GLU 54:  iCode=' ', ILE 57:  iCode=' ' helix 1) packing angle 103.734
3) 17 (LEU 20: , iCode=' ', helix 0) type 4    (hole:  LEU 53:  iCode=' ', GLU 56:  iCode=' ', ILE 57:  iCode=' ', LEU 60:  iCode=' ' helix 1) packing angle 18.443
knobs in helix 1:
4) 29 (LEU 46: , iCode=' ', helix 1) type 4    (hole: LEU 6: iCode=' ', LYS 9: iCode=' ', ASN 10:  iCode=' ', LEU 13:  iCode=' ' helix 0) packing angle 94.014
5) 33 (ILE 50: , iCode=' ', helix 1) type 3    (hole: LYS 9: iCode=' ', ALA 12: iCode=' ', LEU 13:  iCode=' ', LYS 16:  iCode=' ' helix 0) packing angle 25.780
6) 36 (LEU 53: , iCode=' ', helix 1) type 4    (hole:  LEU 13:  iCode=' ', LYS 16:  iCode=' ', ASN 17:  iCode=' ', LEU 20:  iCode=' ' helix 0) packing angle 100.720
7) 40 (ILE 57: , iCode=' ', helix 1) type 3    (hole:  LYS 16:  iCode=' ', GLN 19:  iCode=' ', LEU 20:  iCode=' ', LYS 23:  iCode=' ' helix 0) packing angle 15.117
holes in helix 0:
 LEU 6:  iCode=' ', LYS 9:  iCode=' ', ASN 10:  iCode=' ', LEU 13:  iCode=' ' (knob: 29 (LEU 46: , helix 1))
 LYS 9:  iCode=' ', ALA 12:  iCode=' ', LEU 13:  iCode=' ', LYS 16:  iCode=' ' (knob: 33 (ILE 50: , helix 1))
 LEU 13:  iCode=' ', LYS 16:  iCode=' ', ASN 17:  iCode=' ', LEU 20:  iCode=' ' (knob: 36 (LEU 53: , helix 1))
 LYS 16:  iCode=' ', GLN 19:  iCode=' ', LEU 20:  iCode=' ', LYS 23:  iCode=' ' (knob: 40 (ILE 57: , helix 1))
holes in helix 1:
 ILE 43:  iCode=' ', LEU 46:  iCode=' ', GLU 47:  iCode=' ', ILE 50:  iCode=' ' (knob: 6 (LYS 9: , helix 0))
 LEU 46:  iCode=' ', GLU 49:  iCode=' ', ILE 50:  iCode=' ', LEU 53:  iCode=' ' (knob: 10 (LEU 13: , helix 0))
 ILE 50:  iCode=' ', LEU 53:  iCode=' ', GLU 54:  iCode=' ', ILE 57:  iCode=' ' (knob: 13 (LYS 16: , helix 0))
 LEU 53:  iCode=' ', GLU 56:  iCode=' ', ILE 57:  iCode=' ', LEU 60:  iCode=' ' (knob: 17 (LEU 20: , helix 0))

knob   0 (residue 6 = LYS 9:  iCode=' ') type 4 order 2
knob   1 (residue 10 = LEU 13:  iCode=' ') type 4 order 2
knob   2 (residue 13 = LYS 16:  iCode=' ') type 3 order 2
knob   3 (residue 17 = LEU 20:  iCode=' ') type 4 order 2
knob   4 (residue 29 = LEU 46:  iCode=' ') type 4 order 2
knob   5 (residue 33 = ILE 50:  iCode=' ') type 3 order 2
knob   6 (residue 36 = LEU 53:  iCode=' ') type 4 order 2
knob   7 (residue 40 = ILE 57:  iCode=' ') type 3 order 2
knob   8 (residue 43 = LEU 60:  iCode=' ') type 2 order -1
```

```
CC  0:  2 helices   0  1      frequency 4

helix 0 is in a 2-stranded CC
helix 1 is in a 2-stranded CC

CC  0:angle between helices  0 and  1 is   20.356    parallel

assigning heptad to helix 0 (X) 3-28:
extent of CC packing:   6- 23:
sequence IAQLKEKNAALKEKNQQLKEKIQALK
register    abcdefgabcdefgabcd
partner  ------Y---Y--Y---Y--------
knobtype ------4---4--3---4--------
repeats   0 non-canonical interrupts in  18 residues: 7,7,4

assigning heptad to helix 1 (Y) 43-61:
extent of CC packing:  43- 60:
sequence IAALEKEIAALEKEIAALE
register abcdefgabcdefgabcd
partner  ---X---X--X---X--X-
knobtype ---4---3--4---3--2-
repeats   0 non-canonical interrupts in  18 residues: 7,7,4
E3-P1K-MD3.pdb c  8.00 e 0 result 1 CCS PRESENT
Finished
```

## SOCKET analysis of $E_3/P1_K$: Knobs-into-holes exact distances

```
SOCKET v3.02 02-11-01 John Walshaw, University of Sussex
E3-P1K-MD3.pdb helix   0 (chain  ) 3(iCode=' ')..28(iCode=' ')   cutoff    7.5
      4 knobs, 4 type 0, 4 type 1, 4 type 2, 4 type 3, 3 type 4, 0 type 5, 0 type
6

E3-P1K-MD3.pdb ILE    3:  iCode=' '
E3-P1K-MD3.pdb ALA    4:  iCode=' '
E3-P1K-MD3.pdb GLN    5:  iCode=' '
E3-P1K-MD3.pdb LEU    6:  iCode=' 'Ra[2p]
E3-P1K-MD3.pdb LYS    7:  iCode=' 'Rb[2p]
E3-P1K-MD3.pdb GLU    8:  iCode=' 'Rc[2p]
E3-P1K-MD3.pdb LYS    9:  iCode=' 'Rd[2p] T4 H  1:  93.250 ; hole (adea) chain
 :  (0) ILE   43' '    5.634 (1) LEU   46' '    6.579 (2) GLU   47' '    4.941
(3) ILE   50' '    5.852; sides 0-1:   6.715, 0-2:   6.770, 1-3:   7.645, 2-3:
  7.165
E3-P1K-MD3.pdb ASN   10:  iCode=' 'Re[2p]
E3-P1K-MD3.pdb ALA   11:  iCode=' 'Rf[2p]
E3-P1K-MD3.pdb ALA   12:  iCode=' 'Rg[2p]
E3-P1K-MD3.pdb LEU   13:  iCode=' 'Ra[2p] T4 H  1:  24.518 ; hole (dgad) chain
 :  (0) LEU   46' '    5.824 (1) GLU   49' '    5.969 (2) ILE   50' '    5.463
(3) LEU   53' '    5.385; sides 0-1:   7.509, 0-2:   7.645, 1-3:   6.913, 2-3:
  6.816
E3-P1K-MD3.pdb LYS   14:  iCode=' 'Rb[2p]
E3-P1K-MD3.pdb GLU   15:  iCode=' 'Rc[2p]
E3-P1K-MD3.pdb LYS   16:  iCode=' 'Rd[2p] T3 H  1: 103.734 ; hole (adea) chain
 :  (0) ILE   50' '    5.790 (1) LEU   53' '    7.116 (2) GLU   54' '    4.184
(3) ILE   57' '    6.469; sides 0-1:   6.816, 0-2:   6.608, 1-3:   8.099, 2-3:
  6.730
E3-P1K-MD3.pdb ASN   17:  iCode=' 'Re[2p]
E3-P1K-MD3.pdb GLN   18:  iCode=' 'Rf[2p]
E3-P1K-MD3.pdb GLN   19:  iCode=' 'Rg[2p]
```

```
E3-P1K-MD3.pdb LEU   20:  iCode=' 'Ra[2p] T4 H  1:  18.443 ; hole (dgad) chain
 :  (0) LEU   53' '    5.731 (1) GLU   56' '    5.085 (2) ILE   57' '    5.755
(3) LEU   60' '    6.723; sides 0-1:   7.259, 0-2:   8.099, 1-3:   7.455, 2-3:
  7.710
E3-P1K-MD3.pdb LYS   21:  iCode=' 'Rb[2p]
E3-P1K-MD3.pdb GLU   22:  iCode=' 'Rc[2p]
E3-P1K-MD3.pdb LYS   23:  iCode=' 'Rd[2p]
E3-P1K-MD3.pdb ILE   24:  iCode=' '
E3-P1K-MD3.pdb GLN   25:  iCode=' '
E3-P1K-MD3.pdb ALA   26:  iCode=' '
E3-P1K-MD3.pdb LEU   27:  iCode=' '
E3-P1K-MD3.pdb LYS   28:  iCode=' '

E3-P1K-MD3.pdb helix    1 (chain  ) 43(iCode=' ')..61(iCode=' ')  cutoff    7.5
      5 knobs, 5 type 0, 5 type 1, 5 type 2, 4 type 3, 2 type 4, 0 type 5, 0 type
6
E3-P1K-MD3.pdb ILE   43:  iCode=' 'Ra[2p]
E3-P1K-MD3.pdb ALA   44:  iCode=' 'Rb[2p]
E3-P1K-MD3.pdb ALA   45:  iCode=' 'Rc[2p]
E3-P1K-MD3.pdb LEU   46:  iCode=' 'Rd[2p] T4 H  0:  94.014 ; hole (adea) chain
 :  (0) LEU    6' '    5.669 (1) LYS    9' '    6.579 (2) ASN   10' '    5.971
(3) LEU   13' '    5.824; sides 0-1:   8.913, 0-2:   6.670, 1-3:   8.824, 2-3:
  6.974
E3-P1K-MD3.pdb GLU   47:  iCode=' 'Re[2p]
E3-P1K-MD3.pdb LYS   48:  iCode=' 'Rf[2p]
E3-P1K-MD3.pdb GLU   49:  iCode=' 'Rg[2p]
E3-P1K-MD3.pdb ILE   50:  iCode=' 'Ra[2p] T3 H  0:  25.780 ; hole (dgad) chain
 :  (0) LYS    9' '    5.852 (1) ALA   12' '    5.075 (2) LEU   13' '    5.463
(3) LYS   16' '    5.790; sides 0-1:   5.898, 0-2:   8.824, 1-3:   6.447, 2-3:
  8.741
E3-P1K-MD3.pdb ALA   51:  iCode=' 'Rb[2p]
E3-P1K-MD3.pdb ALA   52:  iCode=' 'Rc[2p]
E3-P1K-MD3.pdb LEU   53:  iCode=' 'Rd[2p] T4 H  0: 100.720 ; hole (adea) chain
 :  (0) LEU   13' '    5.385 (1) LYS   16' '    7.116 (2) ASN   17' '    6.076
(3) LEU   20' '    5.731; sides 0-1:   8.741, 0-2:   7.254, 1-3:   9.382, 2-3:
  7.526
E3-P1K-MD3.pdb GLU   54:  iCode=' 'Re[2p]
E3-P1K-MD3.pdb LYS   55:  iCode=' 'Rf[2p]
E3-P1K-MD3.pdb GLU   56:  iCode=' 'Rg[2p]
E3-P1K-MD3.pdb ILE   57:  iCode=' 'Ra[2p] T3 H  0:  15.117 ; hole (dgad) chain
 :  (0) LYS   16' '    6.469 (1) GLN   19' '    7.228 (2) LEU   20' '    5.755
(3) LYS   23' '    4.857; sides 0-1:   7.226, 0-2:   9.382, 1-3:   8.096, 2-3:
  7.591
E3-P1K-MD3.pdb ALA   58:  iCode=' 'Rb[2p]
E3-P1K-MD3.pdb ALA   59:  iCode=' 'Rc[2p]
E3-P1K-MD3.pdb LEU   60:  iCode=' 'Rd[2p] T2 H  0: 116.983 ; hole (ad  ) chain
 :  (0) LEU   20' '    6.723 (1) LYS   23' '    5.814 (2) ILE   24' '    6.361
(3) LEU   27' '    4.853; sides 0-1:   7.591, 0-2:   6.120, 1-3:   8.316, 2-3:
  6.359
E3-P1K-MD3.pdb GLU   61:  iCode=' '
```

## References


1. Cubberley, M. S. & Iverson, B. L. (2001). 1H NMR investigation of solvent effects in aromatic stacking interactions. *J. Am. Chem. Soc. 123*, 7560–7563

2. Shirude, P. S., Kumar, V. a. & Ganesh, K. N. (2005). BisPNA Targeting to DNA: Effect of Neutral Loop on DNA Duplex Strand Invasion byaepPNA-N7G/aepPNA-C Substituted Peptide Nucleic Acids. *European J. Org. Chem. 2005*, 5207–5215

3. Daudey, G. A., Zope, H. R., Voskuhl, J., Kros, A. & Boyle, A. L. (2017). Membrane-Fusogen Distance Is Critical for Efficient Coiled-Coil-Peptide-Mediated Liposome Fusion. *Langmuir 33*, 12443–12452

4. Robson Marsden, H., Elbers, N. A., Bomans, P. H. H., Sommerdijk, N. A. J. M. & Kros, A. (2009). A Reduced SNARE Model for Membrane Fusion. *Angew. Chemie Int. Ed. 48*, 2330–2333

5. Lacroix, E., Viguera, A. R. & Serrano, L. (1998). Elucidating the folding problem of α-helices: local motifs, long-range electrostatics, ionic-strength dependence and prediction of NMR parameters 1 1Edited by A. R. Fersht. *J. Mol. Biol. 284*, 173–191

6. Oshea, E. K., Lumb, K. J. & Kim, P. S. (1993). Peptide Velcro - Design of a Heterodimeric Coiled-Coil. *Curr. Biol. 3*, 658–667

7. Rabe, M., Boyle, A., Zope, H. R., Versluis, F. & Kros, A. (2015). Determination of Oligomeric States of Peptide Complexes Using Thermal Unfolding Curves. *Biopolymers 104*, 65–72

8. Lindhout, D. A., Litowski, J. R., Mercier, P., Hodges, R. S. & Sykes, B. D. (2004). NMR solution structure of a highly stable de novo heterodimeric coiled-coil. *Biopolymers 75*, 367–375

9. L DeLano, W. (2002). Pymol: An open-source molecular graphics tool. *{CCP4} Newsl. Protein Crystallogr. 40*, 1–8

10. Van Der Spoel, D., Lindahl, E., Hess, B., Groenhof, G., Mark, A. E. & Berendsen, H. J. C. (2005). GROMACS: Fast, flexible, and free. *J. Comput. Chem. 26*, 1701–1718

11. Huang, J. & Mackerell, A. D. (2013). CHARMM36 all-atom additive protein force field: Validation based on comparison to NMR data. *J. Comput. Chem. 34*, 2135–2145

12. Tironi, I. G., Sperb, R., Smith, P. E. & Van Gunsteren, W. F. (1995). A generalized reaction field method for molecular dynamics simulations. *J. Chem. Phys. 102*, 5451–5459

13. Hess, B., Bekker, H., Berendsen, H. J. C. & Fraaije, J. G. E. M. (1997). LINCS: A Linear Constraint Solver for molecular simulations. *J. Comput. Chem. 18*, 1463–1472

14. Essmann, U., Perera, L., Berkowitz, M. L., Darden, T., Lee, H. & Pedersen, L. G. (1995). A smooth particle mesh Ewald method. *J. Chem. Phys. 103*, 8577–8593

15. Birdsall, C. K. & Langdon, A. . (CRC Press, 2018). *Plasma Physics via Computer Simulation*.

16. Fliege1, J. È. & Fux, B. (2000). *Steepest descent methods for multicriteria optimization*. *Math Meth Oper Res*

17. Evans, D. J. & Holian, B. L. (1985). The Nose-Hoover thermostat. *J. Chem. Phys. 83*, 4069–4074

18. Parrinello, M. & Rahman, A. (1981). Polymorphic transitions in single crystals: A new molecular dynamics method. *J. Appl. Phys. 52*, 7182–7190